



UNIVERSITÀ DEGLI STUDI DI TRENTO

Department of Industrial Engineering

Master's degree in *Mechatronics Engineering*

Course of Mechanical vibrations

Laboratory experience

LATERAL VIBRATIONS OF A BEAM

Professors:

Daniele Bortoluzzi
Davide Vignotto

Students:

Giorgio Checola

Academic Year 2019 - 2020

Introduction

This report concerns the laboratory experience of year 2019-2020. We studied the behaviour of a beam when it is excited by forces and observed the lateral vibrations that are generated during different tests. We used accelerometers, in different positions of the beam, to acquire data, which are the accelerations produced by the excitation. The picture below shows the scheme of the analytical model of the system: as you can see, it is blocked from two pins at both ends.

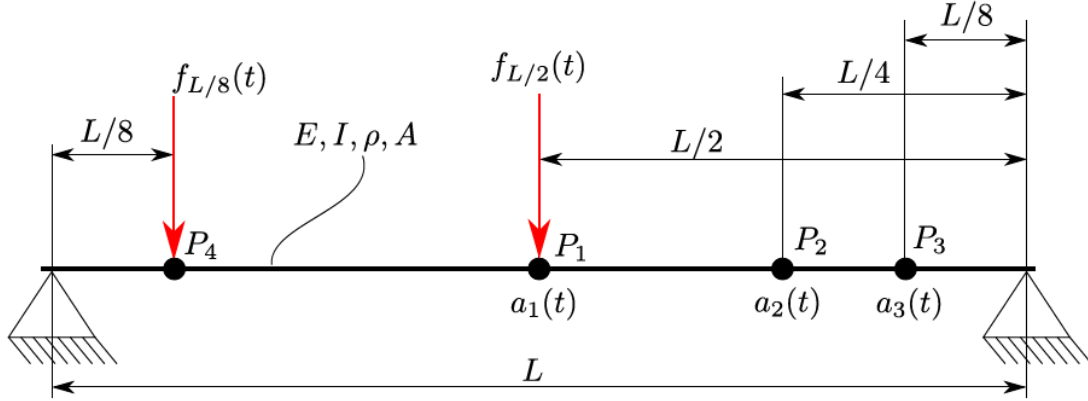


Figure 1: Model of the beam

Before starting with the experimental part, it has been necessary to build the analytical model of the beam, for which we used these parameter values:

Name	Value	Unit	Description
E	206	GPa	Young modulus
ρ	7850	$\frac{kg}{m^3}$	mass density
A	111	mm^2	area of the beam cross-section
I	6370	mm^4	moment of inertia of the beam cross-section
L	0.7	m	length of the beam
ξ_1	0.05	-	damping ratio of the first mode
$\xi_{2,3,4}$	0.01	-	damping ratio of the second, third and fourth mode

Table 1: Parameters of the beam

1 Analytical model

In this part of the project I preferred to use Maple since it is useful for analytic calculations and symbolic computation.

1. As reference frame of the system I chose the left pin to be practical.

In order to find the values of the first five natural frequencies I followed the procedure explained in class.

- Starting from the definition of displacement $W(x)$ and momentum $M(x)$ (we exploit the separation of variable and consider the free vibration of a uniform beam):

$$W(x) = c_1 \cos(\beta x) + c_2 \sin(\beta x) + c_3 \cosh(\beta x) + c_4 \sinh(\beta x)$$

$$M(x) = EI \frac{d^2 W}{dx^2}, \quad \beta = \omega_n^2 \frac{\rho A}{EI}$$

- Writing the boundary conditions for a pinned-pinned beam:

$$\begin{aligned} \rightarrow W(0) &= 0 & \rightarrow W(L) &= 0 \\ \rightarrow M(0) &= 0 & \rightarrow M(L) &= 0 \end{aligned}$$

In both joints there is no possibility to have a lateral displacement, moreover the beam is free to rotate, and so there is no external action that tends to keep the beam fixed. Finally we obtained:

$$\left[\begin{array}{c} c_1 + c_3 = 0 \\ -EI\beta^2 (c_1 - c_3) = 0 \\ c_1 \cos(\beta L) + c_2 \sin(\beta L) + c_3 \cosh(\beta L) + c_4 \sinh(\beta L) = 0 \\ -EI\beta^2 (c_1 \cos(\beta L) + c_2 \sin(\beta L) - c_3 \cosh(\beta L) - c_4 \sinh(\beta L)) = 0 \end{array} \right]$$

- Solving the equations to get the constants and the values of β which satisfy the equalities: I got c_1 and c_3 that are equal to 0 and substituted their values in the other two equations which I wrote in matrix form.

$$\left[\begin{array}{cc} \sin(\beta L) & \sinh(\beta L) \\ -EI\beta^2 \sin(\beta L) & EI\beta^2 \sinh(\beta L) \end{array} \right] \begin{bmatrix} c_2 \\ c_4 \end{bmatrix} = \begin{bmatrix} 0 \\ 0 \end{bmatrix}$$

I want non trivial solution, so I imposed the determinant of the 2x2 matrix equal to 0 and solved for β .

$$2\beta^2 \sin(\beta L) EI \sinh(\beta L) = 0 \quad (1)$$

I took the first five values of the real solutions of β since I want only the first five natural frequencies. By knowing that $\omega_n = \beta^2 \sqrt{\frac{EI}{\rho A}}$ I found these values and relative frequencies:

n°	1	2	3	2	2
ω_n [rad/s]	781.6470157	3126.588063	7034.823141	12506.35225	19541.17539
f [Hz]	124.4029863	497.6119452	1119.626877	1990.447781	3110.074658

Table 2: Values of the first five natural frequencies and related frequencies

For mode shapes I used the third boundary condition equation substituting one of the β values (the solutions do not change). You can see that $c_4 = 0$, then I chose $c_2 = 1$ otherwise every constants would have been null. Finally I obtained the first five mode shapes that I was searching for, shown in the figure below.

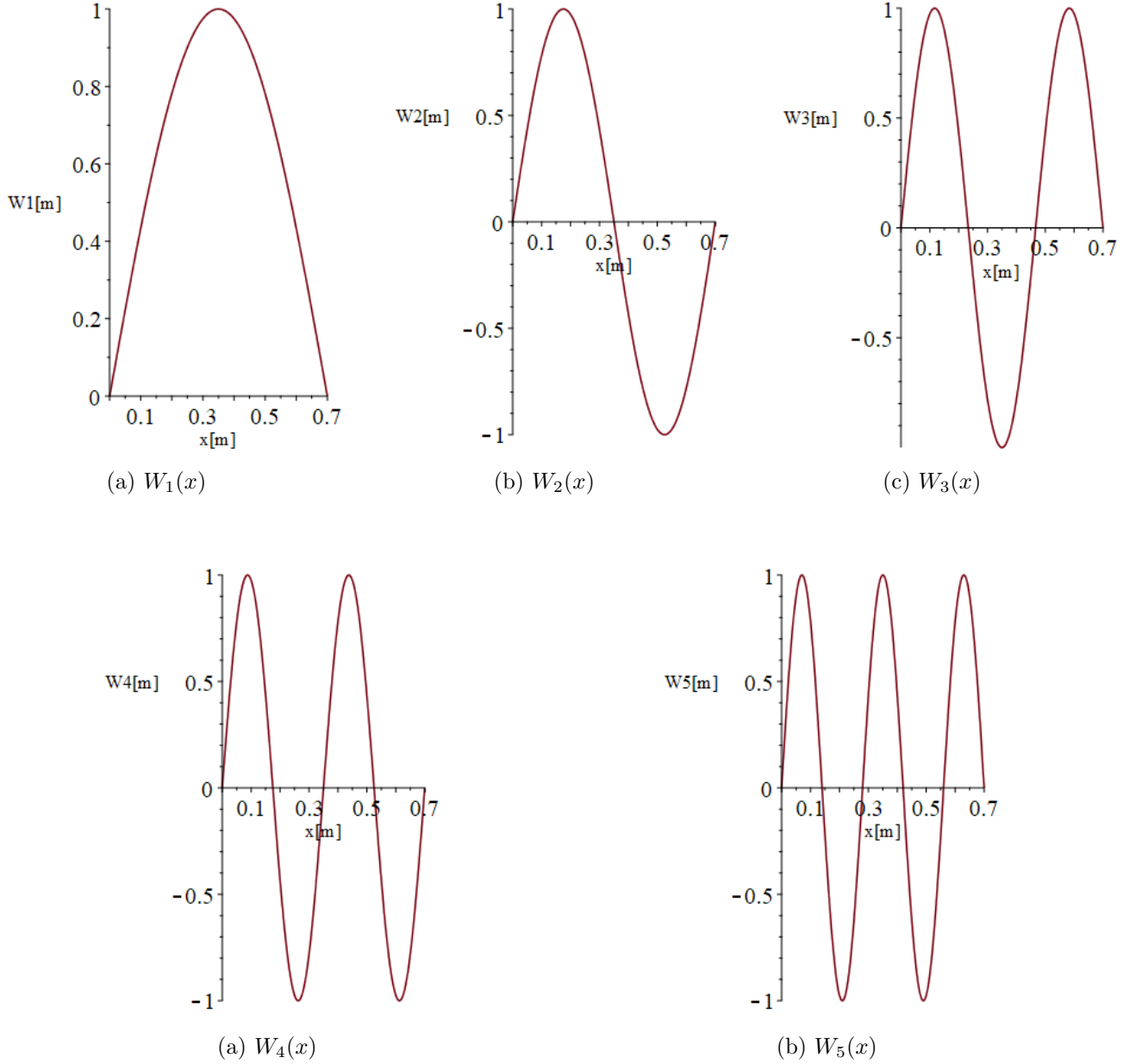


Figure 3: First five mode shapes of the pinned-pinned beam

2. Using the mode superposition principle and exploiting the orthogonality of modal shapes, I built the analytical model of the pinned-pinned beam including also the damping factor. I need to approximate the motion of the system accordingly to Eq 1.

$$w(x, t) = \sum_{n=1}^{\infty} W_n(x) q_n(t) \approx \sum_{n=1}^4 W_n(x) q_n(t) \quad (2)$$

Let's consider the forced vibrations of the beam: I firstly computed the two external force $f(x,t)$ in P_1 and P_4 :

$$(a) \quad f(x,t) = \delta(x - \frac{L}{2})h(t)$$

$$(b) \quad f(x,t) = \delta(x - \frac{L}{8})h(t)$$

where $\frac{L}{2}$ and $\frac{L}{8}$ are the distances of the points of application of the two forces from the left pin.

Then I found the related modal component $Q_m(t)$ truncated at the forth modal shapes and the modal mass b_m using the formulas:

$$Q_m = \int_0^L W_m f(x,t) dx$$

$$b_m = \int_0^L W_m^2 dx$$

Substituting everything in the modal coordinate equation, I solved it using Laplace Transform with zero initial conditions as a function of $q_n(s)$ (the exact values are shown in the Maple file).

$$\frac{d^2 dq_n}{dt^2} + 2\xi_n \omega_n \frac{dq_n}{dt} + \omega_n^2 q_n = \frac{1}{\rho A b} Q_n \quad (3)$$

$$s^2 q_n(s) + 2\xi_n \omega_n \cdot q_n(s) + \omega_n^2 q_n(s) = \frac{1}{\rho A b} Q_n \quad (4)$$

The results for the force applied in P1:

$$\begin{bmatrix} q_1(s) \\ q_2(s) \\ q_3(s) \\ q_4(s) \end{bmatrix} = \begin{bmatrix} \frac{2h(s)L^3}{2\xi_1 \sqrt{\frac{EI}{\rho A}} \pi^2 s \rho A L^2 + s^2 \rho A L^4 + EI \pi^4} \\ 0 \\ \frac{-2h(s)L^3}{18\xi_3 \sqrt{\frac{EI}{\rho A}} \pi^2 s \rho A L^2 + s^2 \rho A L^4 + 81EI \pi^4} \\ 0 \end{bmatrix}$$

And for the force applied in P4

$$\begin{bmatrix} q_1(s) \\ q_2(s) \\ q_3(s) \\ q_4(s) \end{bmatrix} = \begin{bmatrix} \frac{2h(s) \sin(\frac{\pi}{8}) L^3}{(2\xi_1 \sqrt{\frac{EI}{\rho A}} \pi^2 s \rho A L^2 + s^2 \rho A L^4 + EI \pi^4)} \\ \frac{h(s) \sqrt{2} L^3}{(8\xi_2 \sqrt{\frac{EI}{\rho A}} \pi^2 s \rho A L^2 + s^2 \rho A L^4 + 16EI \pi^4)} \\ \frac{2h(s) \sin(\frac{3\pi}{8}) L^3}{(18\xi_3 \sqrt{\frac{EI}{\rho A}} \pi^2 s \rho A L^2 + s^2 \rho A L^4 + 81EI \pi^4)} \\ \frac{2h(s) L^3}{(32\xi_4 \sqrt{\frac{EI}{\rho A}} \pi^2 s \rho A L^2 + s^2 \rho A L^4 + 256EI \pi^4)} \end{bmatrix}$$

Finally, once obtained $q_n(s)$, I got $w(x,s)$ as desired.

3. In order to compute the analytical transfer function, I divided by $h(s)$ the beam displacement function $w(x,s)$; I substituted the position of the accelerometer, and multiplied by s^2 since I want the relation between an acceleration and a force, not between a position and a force. Since I have 3 accelerometers and 2 forces I got 6 transfer function $H_{ij} = \frac{A_i(s)}{F_j(s)}$.

4. The plot of the different transfer functions are visible in the following figures: s has been replaced by $\iota\omega$ to get the frequency response functions; the frequency range is $20 \div 2230$ Hz.

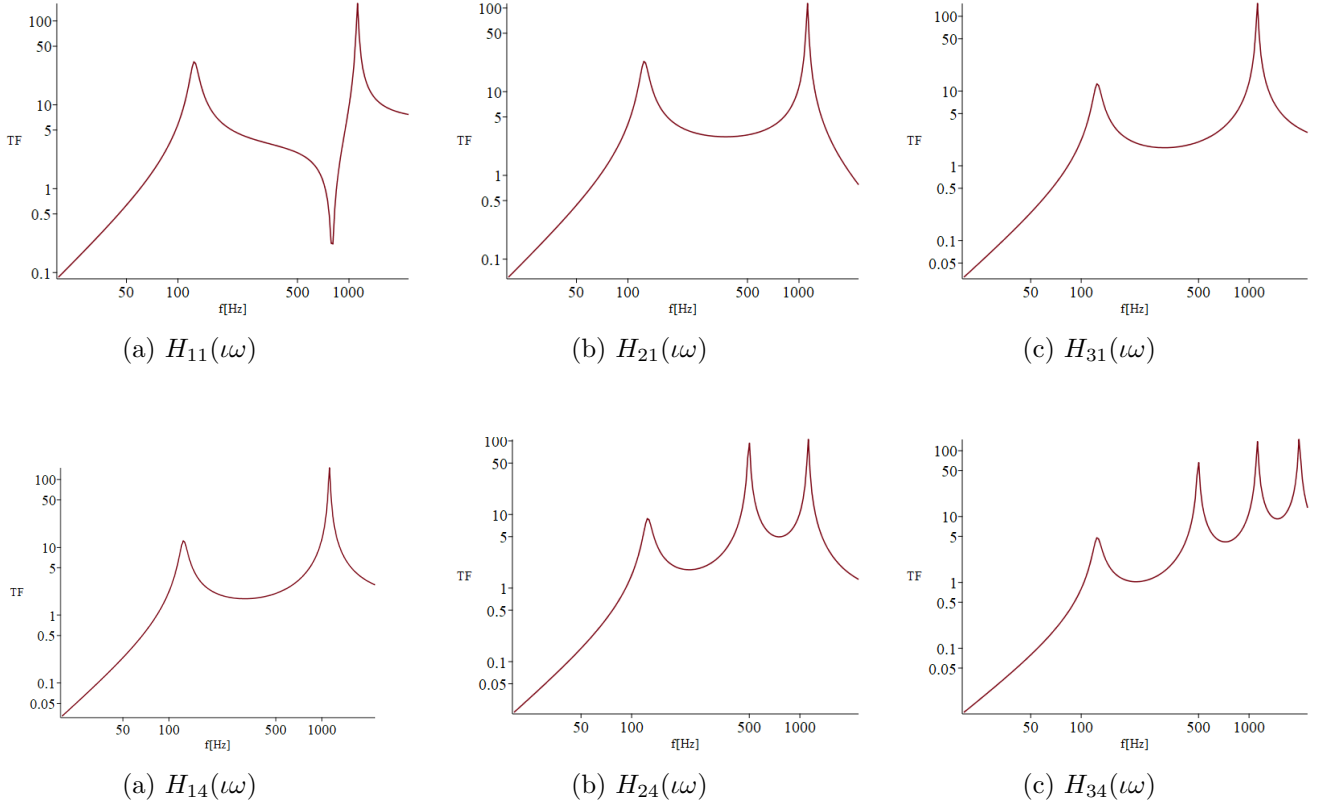


Figure 5: Transfer function $H_{ij}(\iota\omega)$ between force and acceleration, $i = P_1, P_2, P_3$ and $j = P_1, P_4$

Observing carefully, you can see that each plot includes two or more resonant peaks in proximity of the natural frequencies found previously, due to the fact that we computed the transfer function starting from the equation (4) and (2), and so the poles coincide with the natural frequencies of the free vibrations case. The minimal difference could be due to the dissipating term.

Moreover the position of the force and the accelerometers affect the graphs causing peak cancellation if their position coincide with a node.

5. Now let's consider the fixed-fixed beam, with the same characteristics of before.

I want to compute the analytical values of the natural frequencies and numerically evaluate those inside the frequency range of interest f_{range} .

I followed the same procedure of question 1. The boundary conditions are different from before:

$$\rightarrow W(0) = 0$$

$$\rightarrow W(L) = 0$$

$$\rightarrow \frac{dW}{dx}(0) = 0$$

$$\rightarrow \frac{dW}{dx}(L) = 0$$

In this case $c1$ and $c2$ are not 0, but they are function of $c3$ and $c4$; I substitute them in the other two equations; I tried to solve the determinant but there are no analytical valid solutions. Therefore I did it numerically with the function `fsolve` taking the first five values of β and finally I computed natural frequencies and their corresponding Hz values, and see if they lie inside the range.

n°	1	2	3	2	2
ω_n [rad/s]	1771.906055	4884.327263	9575.234362	15828.34881	23644.82237
f [Hz]	282.0076073	777.3648276	1523.945880	2519.159954	3763.190357

Table 3: Values of the first five natural frequencies and related frequencies

You can see that only the first 3 are inside the range. Then I found the relationship between c_3 and c_4 , chose $c_4 = 1$ as reference, and found the relative c_3 values. Finally I obtained the plots of mode shapes.

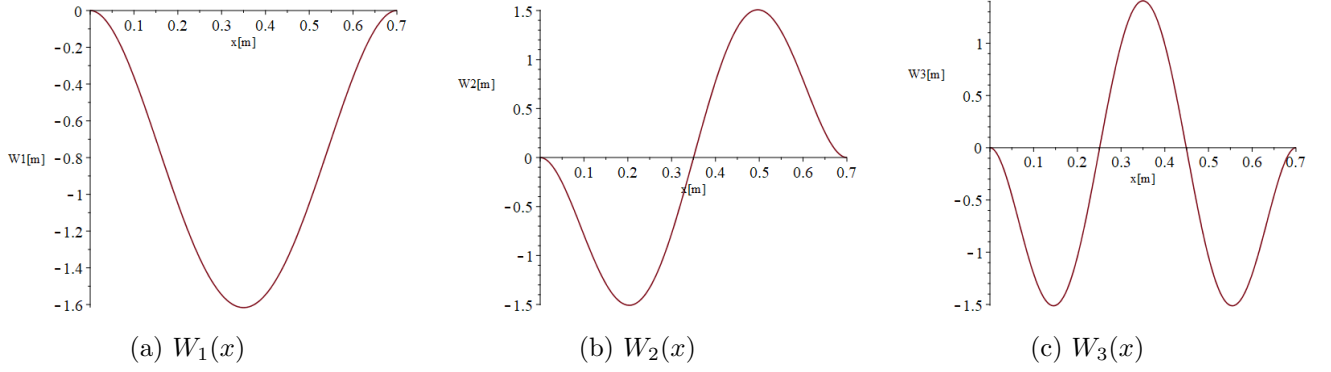


Figure 6: First three mode shapes of fixed-fixed beam

2 Noise analysis

Once concluded the analytical model of the system, I went on to the experiment. In this part the noise affecting the measurements was collected. There are no external force.

The data that we are interested in are: time(s), force(N), acceleration of accelerometer 1 (m/s^2), acceleration of accelerometer 2 (m/s^2), acceleration of accelerometer 3 (m/s^2)

1. In the figures below data of accelerations measured by the accelerometers are plotted as functions of time during the 20 sec.

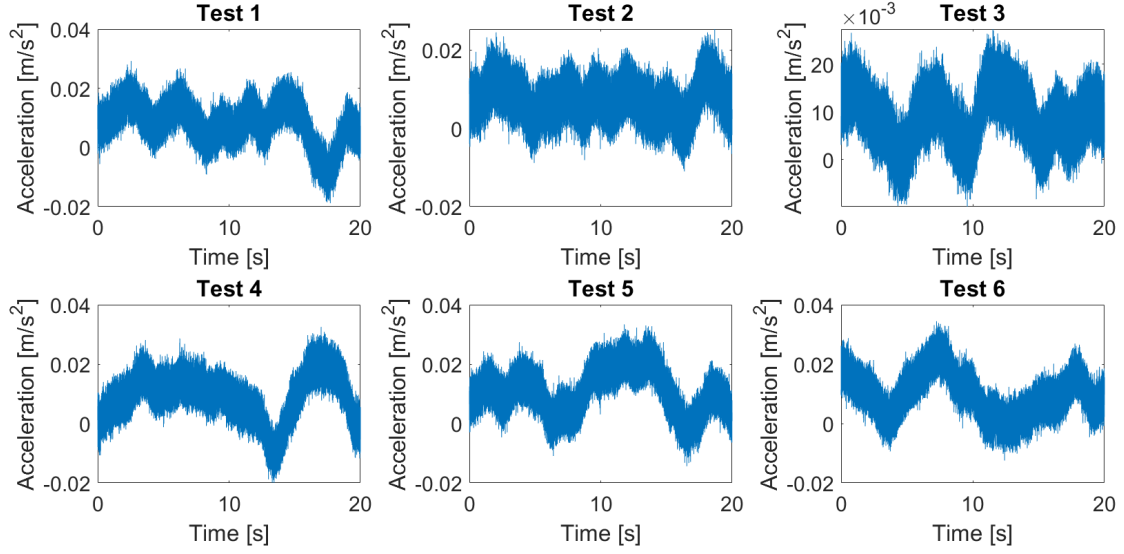


Figure 7: Data from accelerometer 1

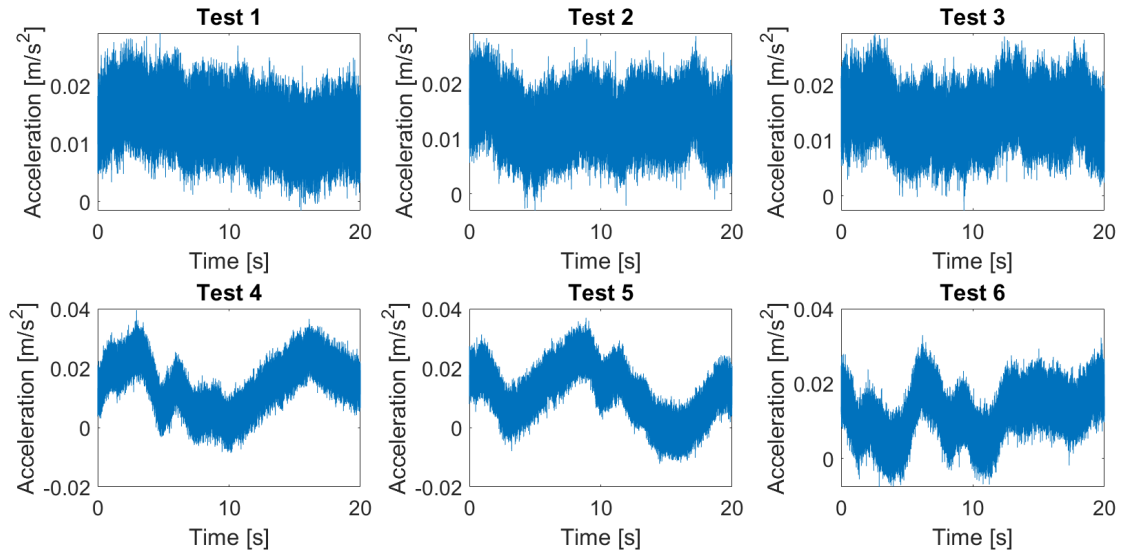


Figure 8: Data from accelerometer 2

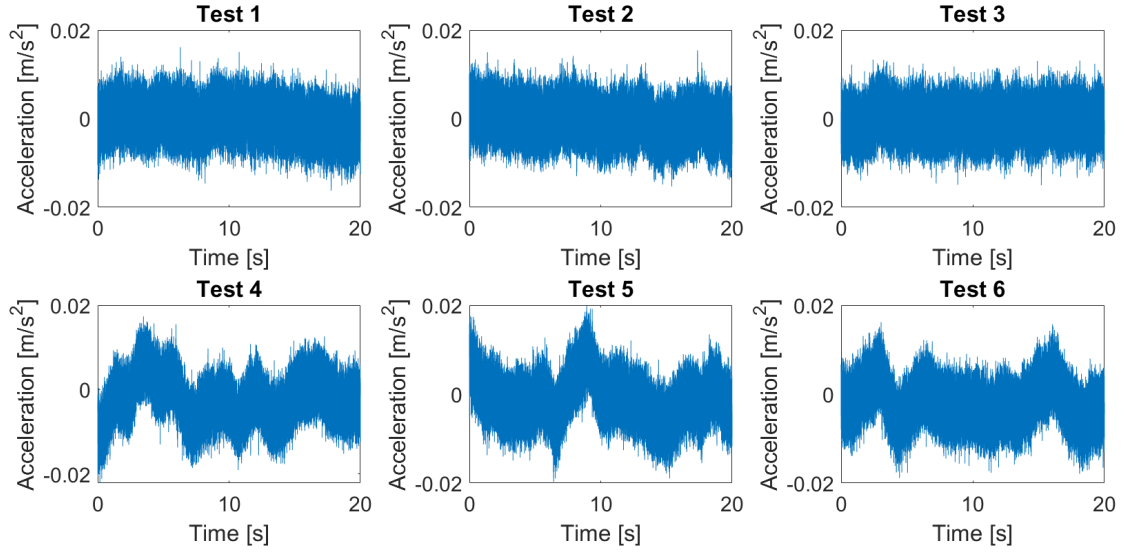


Figure 9: Data from accelerometer 3

These values of noise are quite low. As we will see, they do not affect on the next experiments.

2. In order to find the power spectral density of each curve, I followed the general procedure starting computing FFT (Fast Fourier Transform). I calculated the PSD (Power Spectral Density) non squared because the squared one would have produced a too small signal to be handle by MATLAB.

I also took the mean among the six tests and the standard deviation so that I could plot them together.

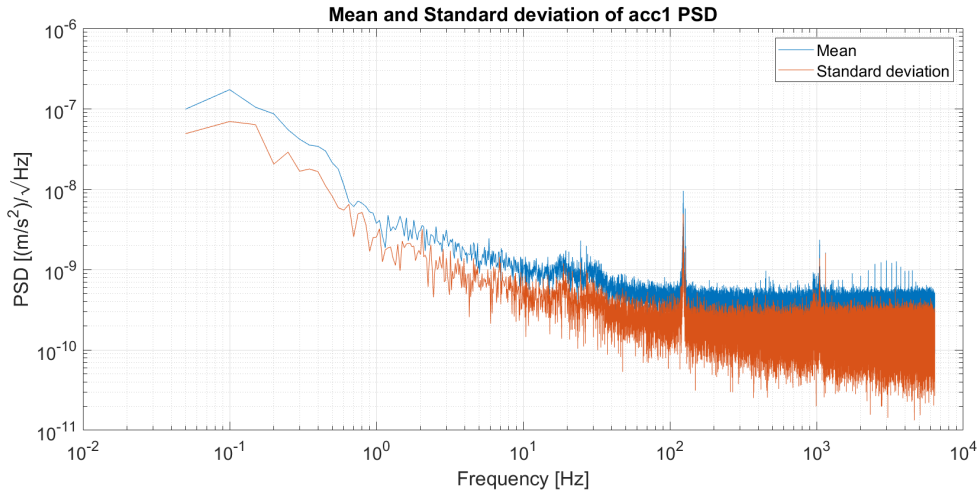


Figure 10: PSD of accelerometer 1

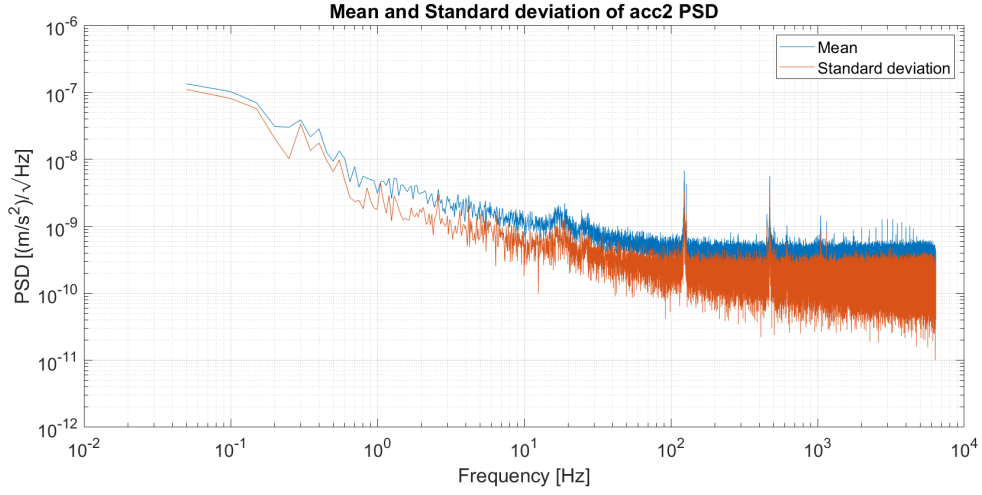


Figure 11: PSD of accelerometer 2

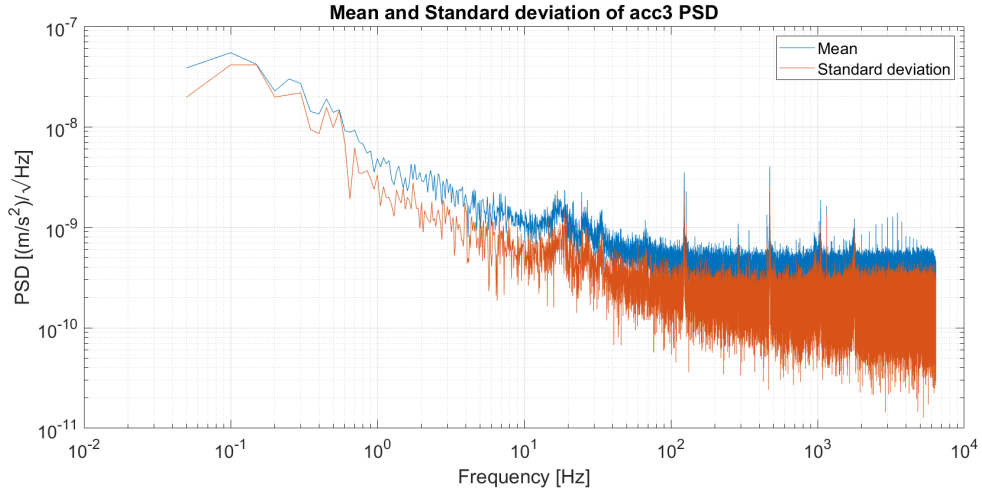


Figure 12: PSD of accelerometer 3

By observing the graphs you can see that there are some peaks along the response. Their locations are closed to the analytical natural frequencies of the pinned-pinned beam. A particularity is that in the signal of the first accelerometer there isn't the peak at the second natural frequency, probably due to the fact that it is located in the node of the related mode shape. This happens also for the other accelerometers for the last three nodes, but with a minor effect.

3 Impact hammer excitation

After analyzing the beam without input, we studied its behavior following an excitation by a impact hammer. The hitting point is P1, located in the middle of the beam.

As previously, force and accelerations have been measured by the instruments.

1. The model of the hammer is 086C03, and the hardest tip was mounted. By viewing its frequency response, it reaches -3 dB at around 2000 Hz. For this reason the range of interest is $f_{range} = 20 \div 2230$ Hz.

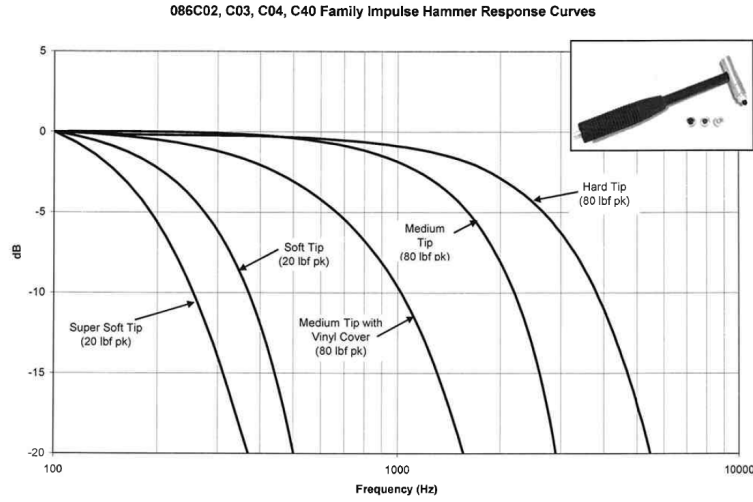


Figure 13: Hammer response curve for different tips

2. The pictures below show the accelerations measured by the three accelerometers in each tests along the time duration.

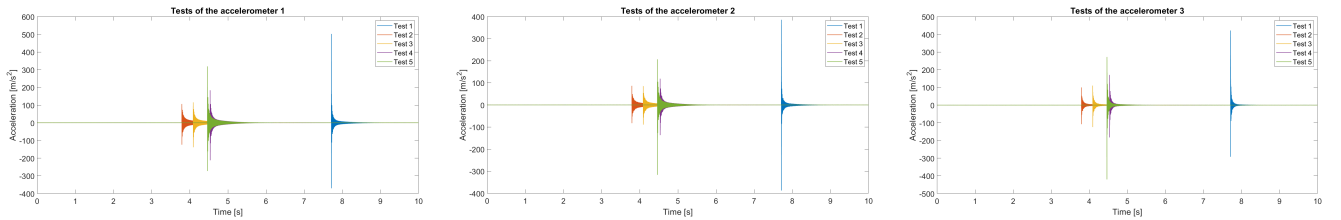


Figure 14: Accelerations measured in all tests

In the first test one accelerometer measures an acceleration of around 500 m/s^2 . Since the maximum measurable acceleration is $\pm 490 \text{ m/s}^2$, this test must be discarded. Here below I show the difference between this test and a valid one (for example the last).

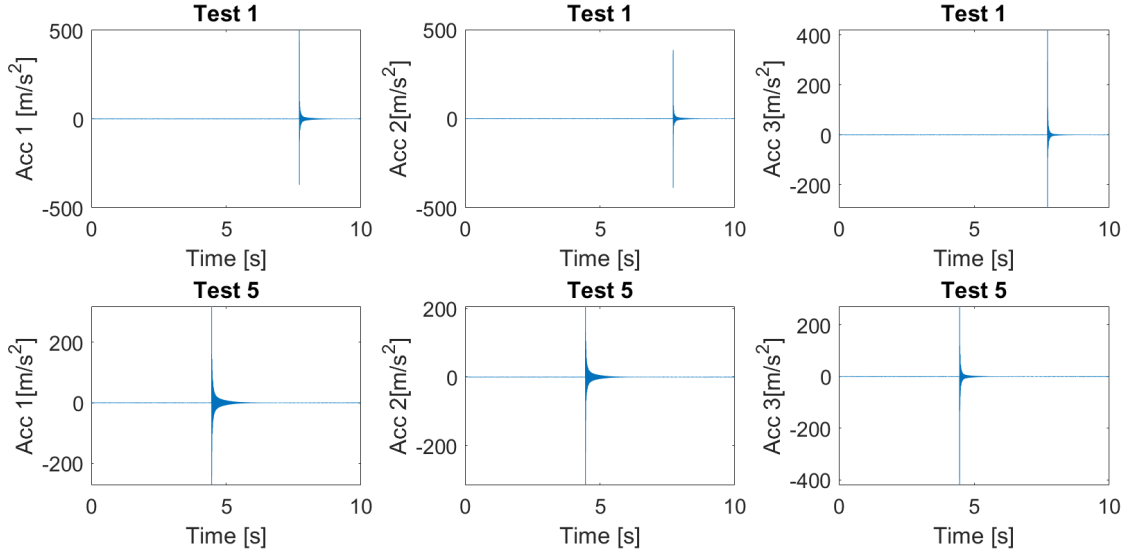


Figure 15: Comparison between the first and the last test

3. From now on, only the valid test will be considered.

I computed the experimental transfer function with the MATLAB function `tfestimate` specifying the input (force) and the output (acceleration). I took the module (with `abs`) to plot the results.

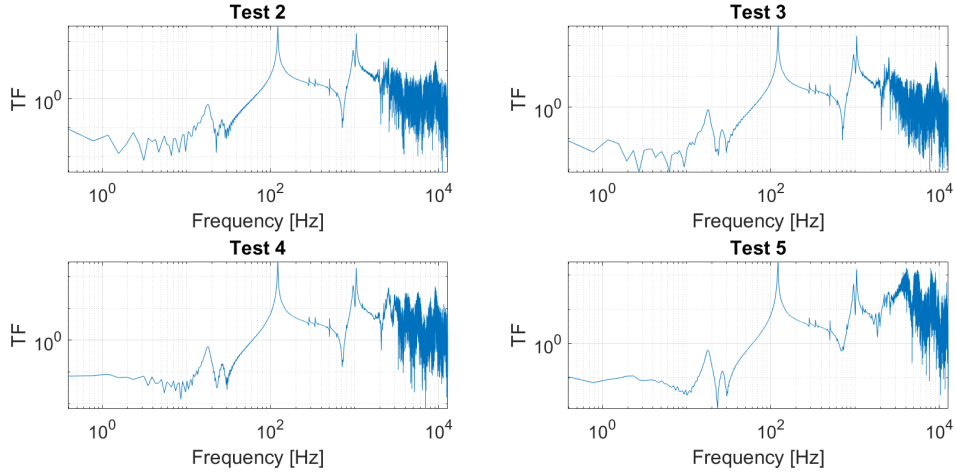


Figure 16: Transfer functions accelerometer 1

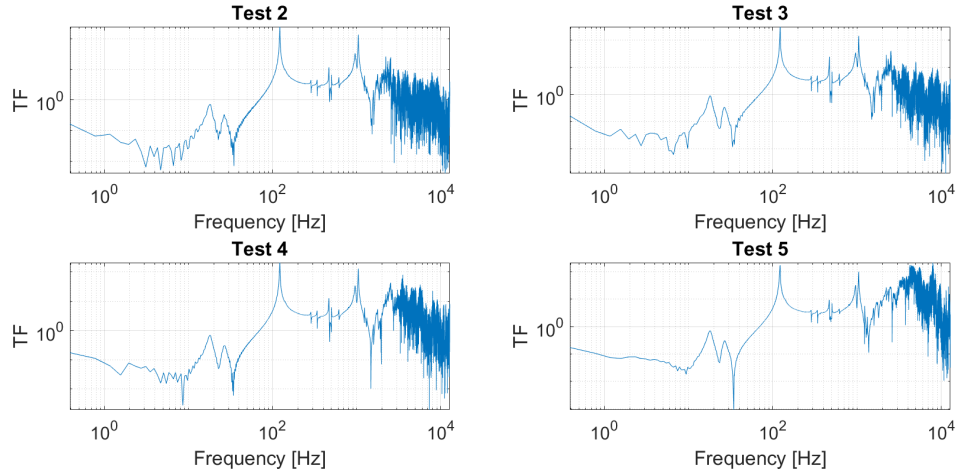


Figure 17: Transfer functions accelerometer 2

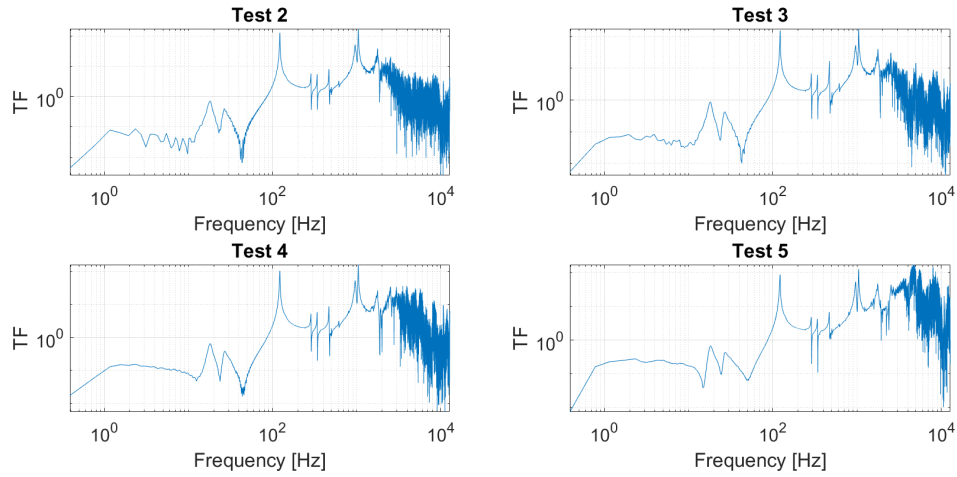


Figure 18: Transfer functions accelerometer 3

4. In the next pictures I compare the analytical TFs (taken by Maple) with the experimental ones.

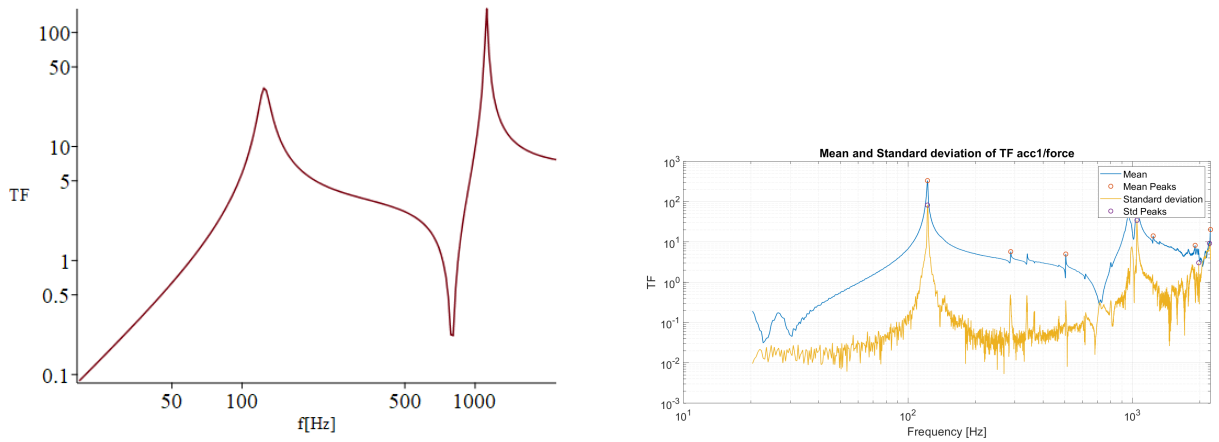


Figure 19: Analytical TF and Experimental TF accelerometer 1 (hammer)

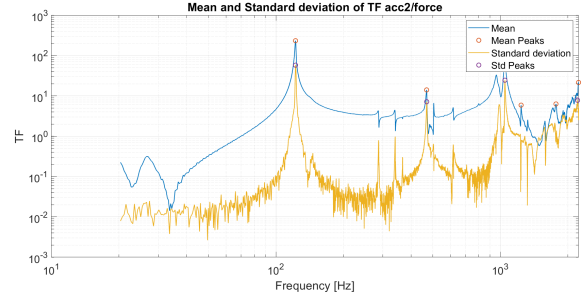
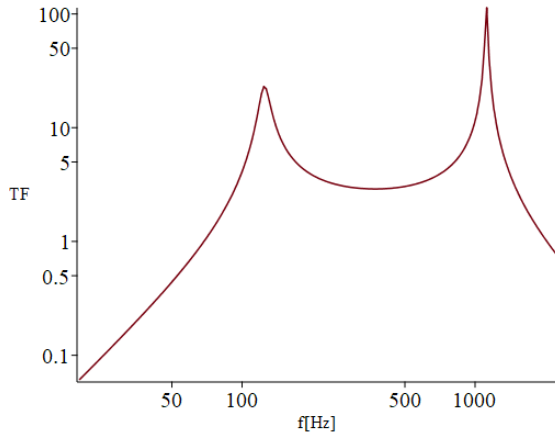


Figure 20: Analytical TF and Experimental TF accelerometer 2 (hammer)

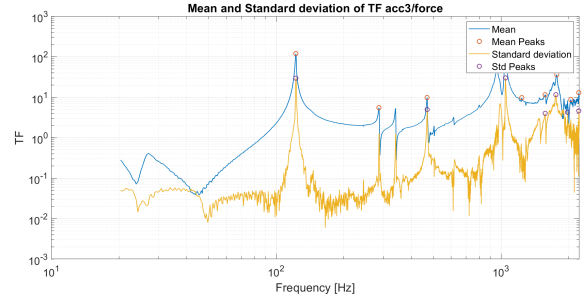
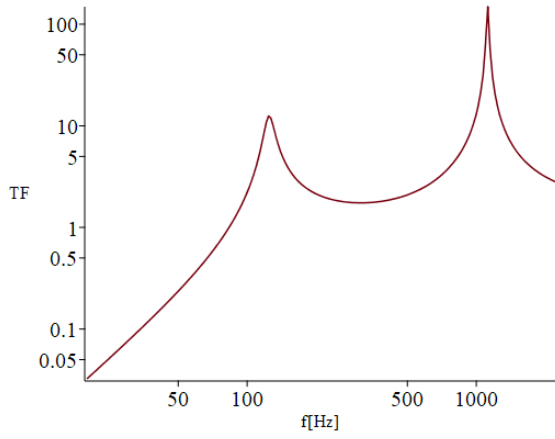


Figure 21: Analytical TF and Experimental TF accelerometer 3 (hammer)

As a first consideration, we can say that the graphs are very similar (with the experimental one less accurate, obviously). The peaks are positioned in proximity of the natural frequencies of the pinned-pinned beam. We can do the comparison with the fixed-fixed beam study: since in a real experiment it's very difficult to recreate an ideal pinned-pinned beam, and so some effects appear in any case: small peaks are visible closed to the natural frequencies of the fixed-fixed beam.

4 Shaker excitation

In this other experiment, the beam is excited with an electro dynamic shaker. The point of application is P_4 , at a distance of $L/8$ from the left pin.

The force is generated as a variable-frequency signal and the excitation has been subdivided in 7 frequency ranges (that cover the overall range of interest $20 \div 2230$ Hz). Each input is repeated 4 times.

Range number	f_{min} (Hz)	f_{max} (Hz)	Duration (s)	Sampl. freq. (Hz)	Repetitions
1	20	430	20	12800	4
2	400	730	20	12800	4
3	700	1030	20	12800	4
4	1000	1330	20	12800	4
5	1300	1630	20	12800	4
6	1600	1930	20	12800	4
7	1900	2230	20	12800	4

Table 4: Frequency ranges used to excite the beam with the shaker

1. Since we have one more variable, we'll have a 4-dimensional matrix of data (just more computationally expensive). The procedure is similar to the previous part but it's necessary to do a for loop more.

I computed the estimate transfer function for each accelerometers, then the mean among four repetition, and the corresponding standard deviation.

2. In order to do a single plot, I had to merge the 7 frequency ranges. We can see below the comparison of the result with the analytical TFs.

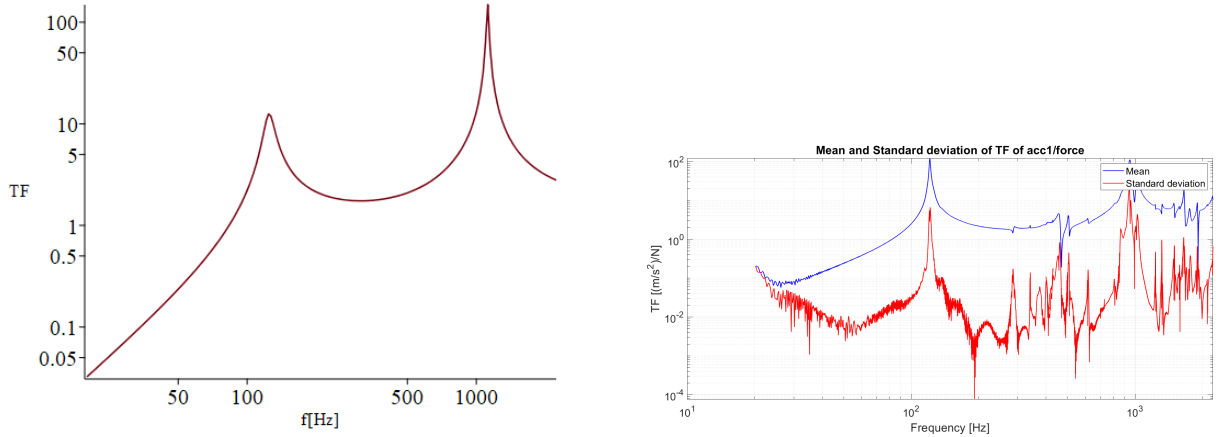


Figure 22: Analytical TF and Experimental TF accelerometer 1 (shaker)

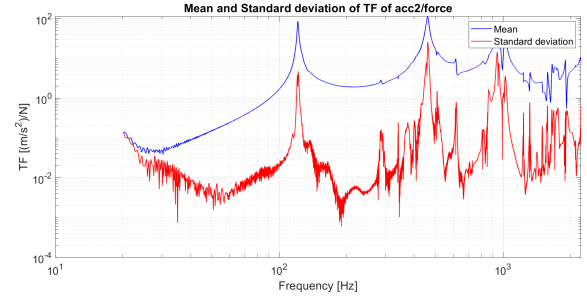
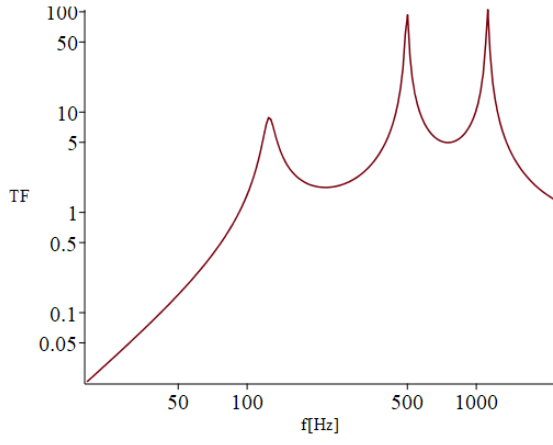


Figure 23: Analytical TF and Experimental TF accelerometer 2 (shaker)

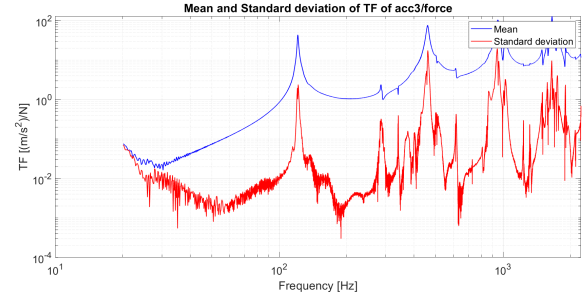
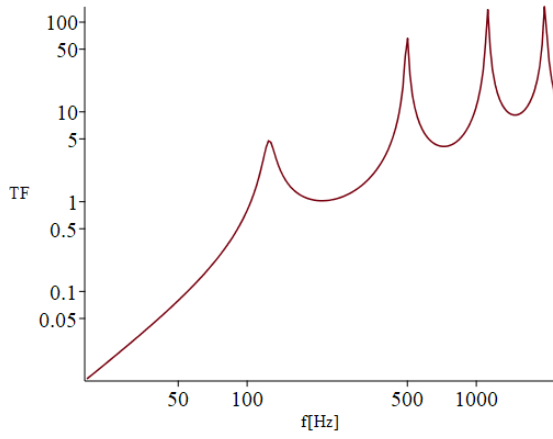


Figure 24: Analytical TF and Experimental TF accelerometer 3 (shaker)

Also in this case the plots are similar and the peaks are in the correct position, closed to the natural frequencies of the pinned-pinned beam.

List of Figures

1	Model of the beam	3
3	First five mode shapes of the pinned-pinned beam	5
5	Transfer function $H_{ij}(\omega)$ between force and acceleration, $i = P_1, P_2, P_3$ and $j = P_1, P_4$	7
6	First three mode shapes of fixed-fixed beam	8
7	Data from accelerometer 1	9
8	Data from accelerometer 2	9
9	Data from accelerometer 3	10
10	PSD of accelerometer 1	10
11	PSD of accelerometer 2	11
12	PSD of accelerometer 3	11
13	Hammer response curve for different tips	12
14	Accelerations measured in all tests	12
15	Comparison between the first and the last test	13
16	Transfer functions accelerometer 1	13
17	Transfer functions accelerometer 2	14
18	Transfer functions accelerometer 3	14
19	Analytical TF and Experimental TF accelerometer 1 (hammer)	14
20	Analytical TF and Experimental TF accelerometer 2 (hammer)	15
21	Analytical TF and Experimental TF accelerometer 3 (hammer)	15
22	Analytical TF and Experimental TF accelerometer 1 (shaker)	16
23	Analytical TF and Experimental TF accelerometer 2 (shaker)	17
24	Analytical TF and Experimental TF accelerometer 3 (shaker)	17

List of Tables

1	Parameters of the beam	3
2	Values of the first five natural frequencies and related frequencies	4
3	Values of the first five natural frequencies and related frequencies	8
4	Frequency ranges used to excite the beam with the shaker	16